

Mesh-robustness of the variable steps BDF2 method for the Cahn-Hilliard model

Hong-lin Liao^{*} Bingquan Ji[†] Lin Wang[‡] Zhimin Zhang[§]

November 19, 2020

Abstract

The two-step backward differential formula (BDF2) implicit method with unequal time-steps is investigated for the Cahn-Hilliard model by focusing on the numerical influences of time-step variations. The suggested method is proved to preserve a modified energy dissipation law at the discrete levels if the adjoint time-step ratios fulfill a new step-ratio restriction $0 < r_k := \tau_k / \tau_{k-1} \leq r_{\text{user}}$ (r_{user} can be chosen by the user such that $r_{\text{user}} < 4.864$), such that it is mesh-robustly stable in an energy norm. We view the BDF2 formula as a convolution approximation of the first time derivative and perform the error analysis by using the recent suggested discrete orthogonal convolution kernels. By developing some novel convolution embedding inequalities with respect to the orthogonal convolution kernels, an L^2 norm error estimate is established at the first time under the updated step-ratio restriction $0 < r_k \leq r_{\text{user}}$. The time-stepping scheme is mesh-robustly convergent in the sense that the convergence constant (prefactor) in the error estimate is independent of the adjoint time-step ratios. On the basis of ample tests on random time meshes, a useful adaptive time-stepping strategy is applied to efficiently capture the multi-scale behaviors and to accelerate the long-time simulation approaching the steady state.

Keywords: Cahn-Hilliard model; adaptive BDF2 method; discrete energy dissipation law; orthogonal convolution kernels, discrete convolution embedding inequality; error estimate

AMS subject classifications. 35Q99, 65M06, 65M12, 74A50

1 Introduction

The Cahn-Hilliard (CH) model is an efficient approach to describe the coarsening dynamics of a binary alloy system [4] and has been applied in other fields including image inpainting [3] and tumor growth [10]. Consider a free energy functional of Ginzburg–Landau type,

$$E[\Phi] = \int_{\Omega} \left[\frac{\epsilon^2}{2} |\nabla \Phi|^2 + F(\Phi) \right] d\mathbf{x} \quad \text{with} \quad F(\Phi) := \frac{1}{4} (\Phi^2 - 1)^2 \quad (1.1)$$

^{*}ORCID 0000-0003-0777-6832; Department of Mathematics, Nanjing University of Aeronautics and Astronautics, Nanjing 211106, P. R. China. Hong-lin Liao (liaohl@nuaa.edu.cn and liaohl@csrc.ac.cn) is supported by a grant 12071216 from National Natural Science Foundation of China.

[†]Department of Mathematics, Nanjing University of Aeronautics and Astronautics, 211101, P. R. China. Bingquan Ji (jibingquanm@163.com).

[‡]Beijing Computational Science Research Center, Beijing 100193, P. R. China. E-mail: wanglin@csrc.ac.cn.

[§]Beijing Computational Science Research Center, Beijing 100193, P. R. China; and Department of Mathematics, Wayne State University, Detroit, MI 48202, USA. E-mails: zmzhang@csrc.ac.cn and ag7761@wayne.edu. This author is supported in part by the NSFC grant 11871092 and NSAF grant U1930402.

where $\mathbf{x} \in \Omega \subseteq \mathbb{R}^2$ and $0 < \epsilon < 1$ is a bounded parameter that is proportional to the interface width. Then the Cahn-Hilliard equation would be given by the H^{-1} gradient flow associated with the free energy functional $E[\phi]$,

$$\partial_t \Phi = \kappa \Delta \mu \quad \text{with} \quad \mu := \frac{\delta E}{\delta \Phi} = F'(\Phi) - \epsilon^2 \Delta \Phi, \quad (1.2)$$

where the parameter κ is the mobility related to the characteristic relaxation time of system and μ is the chemical potential. Assume that Φ is periodic over the domain Ω . By applying the integration by parts, one can find the volume conservation,

$$(\Phi(t), 1) = (\Phi(t_0), 1), \quad (1.3)$$

and the following energy dissipation law,

$$\frac{dE}{dt} = \left(\frac{\delta E}{\delta \Phi}, \partial_t \Phi \right) = (\mu, \Delta \mu) = -\|\nabla \mu\|^2 \leq 0, \quad (1.4)$$

where $(u, v) := \int_{\Omega} uv \, d\mathbf{x}$, and the associated L^2 norm $\|v\| = \sqrt{(v, v)}$ for all $u, v \in L^2(\Omega)$.

The main aim of this paper is to present a rigorous stability and convergence analysis of the BDF2 implicit method with variable time-steps for simulating the CH model (1.2). Consider the nonuniform time levels $0 = t_0 < t_1 < \dots < t_N = T$ with the time-step sizes $\tau_k := t_k - t_{k-1}$ for $1 \leq k \leq N$, and denote the maximum time-step size $\tau := \max_{1 \leq k \leq N} \tau_k$. Let the adjoint time-step ratio $r_k := \tau_k / \tau_{k-1}$ for $2 \leq k \leq N$. Our analysis will focus on the influence of non-uniform time grids (with the associated time-step ratios) on the numerical solution by carefully evaluating the stability and convergence.

This is motivated by the following facts:

- The BDF2 method is A-stable and L-stable such that it would be more suitable than Crank-Nicolson type schemes for solving the stiff dissipative problems, see e.g. [5, 6, 29].
- The nonuniform grid and adaptive time-stepping techniques [13, 18–20, 24] are powerful in capturing the multi-scale behaviors and accelerating the long-time simulations of phase field models including the CH model.
- The convergence theory of variable-steps BDF2 scheme remains incomplete for nonlinear parabolic equations. Actually, the required step-ratio constraint for the L^2 norm stability are severer than the classical zero-stability condition $r_k < 1 + \sqrt{2}$, given by Grigorieff [12]. Always, they contain some undesirable pre-factors $C_r \exp(C_r \Gamma_n)$ or $C_r \exp(C_r t_n)$, see e.g. [2, 8, 11, 17, 28], where Γ_n may be unbounded when certain time-step variations appear and C_r may be infinity as the step-ratios approach the zero-stability limit $1 + \sqrt{2}$.

In our recent works [18, 19, 22], a novel theoretical technique with *discrete orthogonal convolution* (DOC) kernels was suggested to verify that, if the adjoint time-step ratios r_k satisfy a new zero-stability condition [22], that is, $0 < r_k < (3 + \sqrt{17})/2 \approx 3.561$, the variable-steps BDF2 scheme is computationally robust with respect to the time-step variations in simulating linear diffusions [22], the phase field crystal model [18] and the molecular beam epitaxial model without slope selection [19].

Nonetheless, due to the lack of some convolution embedding inequalities with respect to the DOC kernels, the techniques in [18, 19, 22] are inadequate to handle more general nonlinear

problems such as the underlying nonlinear CH model (and Allen-Chan model). The main aim of this paper is to fill this gap by establishing some discrete convolution embedding inequalities with respect to the DOC kernels. Also, the recent analysis in [18, Lemma A.1] with a step-scaled matrix motivates us to update the previous zero-stability restriction in [22] as follows,

S0. $0 < r_k \leq r_{\text{user}} (< 4.864)$ for $2 \leq k \leq N$,

where the value of r_{user} can be chosen in adaptive time-stepping computations by the user such that $r_{\text{user}} < 4.864$, such as $r_{\text{user}} = 2, 3$ or 4 for practical choices. Under the step-ratio constraint **S0**, we will present an L^2 norm error estimate with an improved prefactor, see Theorem 4.1,

$$C_\phi \exp(c_\epsilon t_{n-1}).$$

Here and hereafter, any subscripted C , such as C_u and C_ϕ , denotes a generic positive constant, not necessarily the same at different occurrences; while, any subscripted c , such as $c_\epsilon, c_\Omega, c_p, c_z$ and so on, denotes a fixed constant. The appeared constants may be dependent on the given data (typically, the interface width parameter ϵ) and the solution but are always independent of the spatial lengths, the time t_n , the step sizes τ_n and the step ratios r_n . It is interesting to emphasize that, under the step-ratio constraint **S0**, the involved constants are bounded even when the step-ratios r_n approach the user limit r_{user} such that the variable-steps BDF2 scheme is mesh-robustly convergent.

To the best of our knowledge, this is the first time such an optimal L^2 norm error estimate of variable-steps BDF2 method is established for the Cahn-Hilliard (and Allen-Cahn) type models. As a closely related work, the variable-steps BDF2 scheme for the Allen-Chan equation was also investigated in [20] by using the discrete complementary convolution kernels. The BDF2 scheme was proved to preserve the maximum bound principle if the step-ratios satisfy the classical zero-stability condition $r_k < 1 + \sqrt{2}$. The maximum norm error estimate with a prefactor $\frac{1}{1-\eta} \exp(\frac{t_n}{1-\eta})$ was obtained, where the parameter $\eta \rightarrow 1$ as $\max r_k \rightarrow 1 + \sqrt{2}$. It is to mention that, under the constraint **S0**, one can follow the present analysis to obtain a new L^2 norm error estimate that is robustly stable to the variations of time-steps.

Given a grid function $\{v^k\}_{k=0}^N$, put $\nabla_\tau v^k := v^k - v^{k-1}$, $\partial_\tau v^k := \nabla_\tau v^k / \tau_k$ for $k \geq 1$. Taking $v^n = v(t_n)$, we view the variable-steps BDF2 formula as a discrete convolution summation

$$D_2 v^n := \sum_{k=1}^n b_{n-k}^{(n)} \nabla_\tau v^k \quad \text{for } n \geq 2, \quad (1.5)$$

where the discrete convolution kernels $b_{n-k}^{(n)}$ are defined for $n \geq 2$,

$$b_0^{(n)} := \frac{1 + 2r_n}{\tau_n(1 + r_n)}, \quad b_1^{(n)} := -\frac{r_n^2}{\tau_n(1 + r_n)} \quad \text{and} \quad b_j^{(n)} := 0 \quad \text{for } j \geq 2. \quad (1.6)$$

Without losing the generality, assume that an accurate solution ϕ^1 is available. We consider the stability and convergence of the BDF2 scheme for solving the CH equation (1.2):

$$D_2 \phi^n = \kappa \Delta_h \mu^n \quad \text{with} \quad \mu^n := F'(\phi^n) - \epsilon^2 \Delta_h \phi^n \quad \text{for } 2 \leq n \leq N \quad (1.7)$$

subject to the periodic boundary conditions. The spatial operators are approximated by the Fourier pseudo-spectral method, as described in the next section.

The unique solvability of the BDF2 scheme (1.7) is established in Theorem 2.1 by using the fact that the solution of nonlinear scheme (1.7) is equivalent to the minimization of a convex functional. Lemma 2.1 shows that the BDF2 convolution kernels $b_{n-k}^{(n)}$ are positive definite provided the adjacent time-step ratios r_k satisfy the sufficient condition **S0**. Then we verify in Theorem 2.2 that the adaptive BDF2 time-stepping method (1.7) has a modified energy dissipation law at the discrete levels under a proper step-size constraint.

We are to emphasize that the solution estimates in section 2 are based on the standard form (1.7) of the BDF2 implicit scheme, but in the subsequent L^2 norm error analysis we will use an equivalent convolution form with a class of discrete orthogonal convolution (DOC) kernels. The DOC kernels $\{\theta_{n-k}^{(n)}\}_{k=2}^n$ are defined by (this definition is slightly different from those in [18,19,22] since we do not introduce the discrete kernel $b_0^{(1)}$ for the first-level solver)

$$\theta_0^{(n)} := \frac{1}{b_0^{(n)}} \text{ for } n \geq 2 \quad \text{and} \quad \theta_{n-k}^{(n)} := -\frac{1}{b_0^{(k)}} \sum_{j=k+1}^n \theta_{n-j}^{(n)} b_{j-k}^{(j)} \text{ for } n \geq k+1 \geq 3. \quad (1.8)$$

One has the following discrete orthogonal identity

$$\sum_{j=k}^n \theta_{n-j}^{(n)} b_{j-k}^{(j)} \equiv \delta_{nk} \quad \text{for } 2 \leq k \leq n, \quad (1.9)$$

where δ_{nk} is the Kronecker delta symbol. By exchanging the summation order and using the identity (1.9), it is not difficult to check that

$$\begin{aligned} \sum_{j=2}^n \theta_{n-j}^{(n)} D_2 v^j &= \sum_{j=2}^n \theta_{n-j}^{(n)} b_{j-1}^{(j)} \nabla_\tau v^1 + \sum_{j=2}^n \theta_{n-j}^{(n)} \sum_{\ell=2}^j b_{j-\ell}^{(j)} \nabla_\tau v^\ell \\ &= \theta_{n-2}^{(n)} b_1^{(2)} \nabla_\tau v^1 + \nabla_\tau v^n \quad \text{for } n \geq 2. \end{aligned} \quad (1.10)$$

Acting the DOC kernels $\theta_{m-n}^{(m)}$ on the first equation in (1.7) and summing n from $n = 2$ to m , we apply (1.10) to find the equivalent convolution form (replacing m by n)

$$\nabla_\tau \phi^n = -\theta_{n-2}^{(n)} b_1^{(2)} \nabla_\tau \phi^1 + \kappa \sum_{j=2}^n \theta_{n-j}^{(n)} \Delta_h \mu^j \quad \text{for } 2 \leq n \leq N. \quad (1.11)$$

Note that, by following the proof of [21, Lemma 2.1], we have

$$\sum_{j=k}^m b_{m-j}^{(m)} \theta_{j-k}^{(j)} \equiv \delta_{mk} \quad \text{for } 2 \leq k \leq m. \quad (1.12)$$

With the help of this mutually orthogonal identity, one can recover the original form (1.7) by acting the BDF2 kernels $b_{m-n}^{(m)}$ on the new formulation (1.11). In this sense, the DOC kernels define a *reversible discrete transform* between (1.7) and the convolution form (1.11).

To perform the L^2 norm error analysis, section 3 presents some properties of the DOC kernels $\theta_{n-k}^{(n)}$ and some new convolution embedding inequalities with respect to the DOC kernels, see Lemmas 3.1–3.9. By making use of the H^1 norm solution bound obtained in Lemma 2.2, we establish an optimal L^2 norm error estimate in section 4. Numerical tests and comparisons are presented in section 5 to validate the accuracy and effectiveness of the BDF2 method (1.7), especially when coupled with an adaptive stepping strategy.

2 Solvability and energy dissipation law

We use the same spatial notations in [18]. Set the space domain $\Omega = (0, L)^2$ and consider the uniform length $h_x = h_y = h := L/M$ in each direction for an even positive integer M . Let $\Omega_h := \{\mathbf{x}_h = (ih, jh) \mid 1 \leq i, j \leq M\}$ and put $\bar{\Omega}_h := \Omega_h \cup \partial\Omega$. Denote the space of L -periodic grid functions $\mathbb{V}_h := \{v \mid v = (v_h) \text{ is } L\text{-periodic for } \mathbf{x}_h \in \bar{\Omega}_h\}$.

For a periodic function $v(\mathbf{x})$ on $\bar{\Omega}$, let $P_M : L^2(\Omega) \rightarrow \mathcal{F}_M$ be the standard L^2 projection operator onto the space \mathcal{F}_M , consisting of all trigonometric polynomials of degree up to $M/2$, and $I_M : L^2(\Omega) \rightarrow \mathcal{F}_M$ be the trigonometric interpolation operator [26], i.e.,

$$(P_M v)(\mathbf{x}) = \sum_{\ell, m=-M/2}^{M/2-1} \hat{v}_{\ell, m} e_{\ell, m}(\mathbf{x}), \quad (I_M v)(\mathbf{x}) = \sum_{\ell, m=-M/2}^{M/2-1} \tilde{v}_{\ell, m} e_{\ell, m}(\mathbf{x}),$$

where the complex exponential basis function $e_{\ell, m}(\mathbf{x}) := e^{i\nu(\ell x + m y)}$ with $\nu = 2\pi/L$. The coefficients $\hat{v}_{\ell, m}$ refer to the standard Fourier coefficients of function $v(\mathbf{x})$, and the pseudo-spectral coefficients $\tilde{v}_{\ell, m}$ are determined such that $(I_M v)(\mathbf{x}_h) = v_h$.

The Fourier pseudo-spectral first and second order derivatives of v_h are given by

$$\mathcal{D}_x v_h := \sum_{\ell, m=-M/2}^{M/2-1} (i\nu\ell) \tilde{v}_{\ell, m} e_{\ell, m}(\mathbf{x}_h), \quad \mathcal{D}_x^2 v_h := \sum_{\ell, m=-M/2}^{M/2-1} (i\nu\ell)^2 \tilde{v}_{\ell, m} e_{\ell, m}(\mathbf{x}_h).$$

The differentiation operators \mathcal{D}_y and \mathcal{D}_y^2 can be defined in the similar fashion. In turn, we can define the discrete gradient and Laplacian in the point-wise sense, respectively, by

$$\nabla_h v_h := (\mathcal{D}_x v_h, \mathcal{D}_y v_h)^T \quad \text{and} \quad \Delta_h v_h := \nabla_h \cdot (\nabla_h v_h) = (\mathcal{D}_x^2 + \mathcal{D}_y^2) v_h$$

For any grid functions $v, w \in \mathbb{V}_h$, define the discrete inner product $\langle v, w \rangle := h^2 \sum_{\mathbf{x}_h \in \Omega_h} v_h w_h$, and the associated L^2 norm $\|v\| := \|v\|_{l^2} = \sqrt{\langle v, v \rangle}$. Also, we will use the discrete l^q norm $\|v\|_{l^q} := \sqrt[q]{h^2 \sum_{\mathbf{x}_h \in \Omega_h} |v_h|^q}$ and the H^1 seminorm $\|\nabla_h v\| := \sqrt{h^2 \sum_{\mathbf{x}_h \in \Omega_h} |\nabla_h v_h|^2}$. It is easy to check the discrete Green's formulas, $\langle -\Delta_h v, w \rangle = \langle \nabla_h v, \nabla_h w \rangle$ and $\langle \Delta_h^2 v, w \rangle = \langle \Delta_h v, \Delta_h w \rangle$, see [26] for more details. Also we have the following discrete embedding inequality simulating the Sobolev embedding $H^1(\Omega) \hookrightarrow L^6(\Omega)$,

$$\|v\|_{l^6} \leq c_\Omega (\|v\| + \|\nabla_h v\|) \quad \text{for any } v \in \mathbb{V}_h. \quad (2.1)$$

For the underlying volume-conservative problem, it is also to define a mean-zero function space $\mathring{\mathbb{V}}_h := \{v \in \mathbb{V}_h \mid \langle v, 1 \rangle = 0\} \subset \mathbb{V}_h$. As usual, following the arguments in [26], one can introduce an discrete version of inverse Laplacian operator $(-\Delta_h)^{-\gamma}$ as follows. For a grid function $v \in \mathring{\mathbb{V}}_h$, define

$$(-\Delta_h)^{-\gamma} v_h := \sum_{\substack{\ell, m=-M/2 \\ (\ell, m) \neq \mathbf{0}}}^{M/2-1} (\nu^2 (\ell^2 + m^2))^{-\gamma} \tilde{v}_{\ell, m} e_{\ell, m}(\mathbf{x}_h),$$

and an H^{-1} inner product $\langle v, w \rangle_{-1} := \langle (-\Delta_h)^{-1} v, w \rangle$. The associated H^{-1} norm $\|\cdot\|_{-1}$ can be defined by $\|v\|_{-1} := \sqrt{\langle v, v \rangle_{-1}}$. We have the following Poincaré type inequality with the usual

Poincaré constant c_p , $\|v\|_{-1} \leq c_p \|v\|$, and the generalized Hölder inequality,

$$\|v\|^2 \leq \|\nabla_h v\| \|v\|_{-1} \quad \text{for any } v \in \mathring{V}_h. \quad (2.2)$$

Also the discrete embedding inequality (2.1) can be simplified as ($c_z = c_\Omega + c_\Omega c_p$)

$$\|v\|_{l^6} \leq c_z \|\nabla_h v\| \quad \text{for any } v \in \mathring{V}_h. \quad (2.3)$$

2.1 Unique solvability

To focus on the numerical analysis of the BDF2 solution, it is to assume that

A1. A starting scheme is properly chosen to compute an accurate first-level solution ϕ^1 such that it preserves the initial volume, $\langle \phi^1, 1 \rangle = \langle \phi^0, 1 \rangle = \langle P_M \Phi^0, 1 \rangle$, and also preserves certain (maybe, modified) energy dissipation law. There exists a positive constant c_0 , depended on the domain Ω , the interface parameter ϵ and the initial value ϕ^0 , such that

$$\frac{\epsilon^2}{2} \|\nabla_h \phi^1\|^2 + \langle F(\phi^1), 1 \rangle + \frac{\tau_2}{2\kappa} \|\partial_\tau \phi^1\|_{-1}^2 \leq c_0.$$

Remark 1. Assumption **A1** can be satisfied by many of first-level solvers. The BDF1 scheme would be suited for computing a second-order solution ϕ^1 ; however, a very small initial step τ_1 would not be suggested here since it arrives at a large step-ratio r_2 and eventually affects the accuracy of solution in the whole simulation, see numerical results in [23].

The Crank-Nicolson scheme at the first time-level can generate a second-order difference quotient $\partial_\tau \phi^1$; but a very small initial step τ_1 would not be suggested either because it would be prone to generate nonphysical oscillations. To control possibly initial oscillations, we suggest a special step-ratio $r_2 = \sqrt{2}/2$ in the implementation of our scheme (1.7). Actually, by taking $\phi^\gamma := \phi^1$, $\phi^1 := \phi^2$, $\tau_* := \tau_1 + \tau_2$ and $\gamma := \tau_1/\tau_*$ with $r_2 = 1/\gamma - 1$, the first two steps of (1.7) are equivalent to the following TR-BDF2 method

$$\frac{\phi^\gamma - \phi^0}{\gamma\tau_*} = \frac{\kappa}{2} \Delta_h \mu^\gamma + \frac{\kappa}{2} \Delta_h \mu^0, \quad \frac{2-\gamma}{(1-\gamma)\tau_*} \phi^1 - \frac{1}{\gamma(1-\gamma)\tau_*} \phi^\gamma + \frac{1-\gamma}{\gamma\tau_*} \phi^0 = \kappa \Delta_h \mu^1,$$

which was shown to be L -stable for $\gamma = 2 - \sqrt{2}$, see [15, 27]. Generally, the TR-BDF2 method is defined as a one-step method resulting from the composition of the trapezoidal rule in the first substep, followed by BDF2 formula in the second substep. This combination is empirically justified under the rationale of combining the good accuracy of the trapezoidal rule with the stability and damping of fast modes guaranteed by BDF2 scheme.

The user can also choose other self-starting L -stable schemes, such as the second-order singly-diagonal implicit Runge-Kutta method [1, 14] for $\alpha = (2 - \sqrt{2})/2$,

$$\frac{\phi^\alpha - \phi^0}{\alpha\tau_1} = \kappa \Delta_h \mu^\alpha, \quad \frac{\phi^1 - \phi^0}{\tau_1} = \alpha \kappa \Delta_h \mu^1 + (1 - \alpha) \kappa \Delta_h \mu^\alpha.$$

Under the assumption **A1**, the solution ϕ^n of BDF2 scheme (1.7) preserves the volume, $\langle \phi^n, 1 \rangle = \langle \phi^0, 1 \rangle$ for $n \geq 2$. Actually, taking the inner product of (1.7) by 1 and applying the

summation by parts, one can check that $\langle D_2 \phi^j, 1 \rangle = 0$ for $j \geq 2$. Multiplying both sides of this equality by the DOC kernels $\theta_{n-j}^{(n)}$ and summing the index j from $j = 2$ to n , we get

$$\sum_{j=2}^n \theta_{n-j}^{(n)} \langle D_2 \phi^j, 1 \rangle = 0 \quad \text{for } n \geq 2.$$

It leads to $\langle \nabla_\tau \phi^n, 1 \rangle = 0$ directly by taking $v^j = \phi^j$ in the equality (1.10). Simple induction yields the volume conservation law, $\langle \phi^n, 1 \rangle = \langle \phi^{n-1}, 1 \rangle = \dots = \langle \phi^0, 1 \rangle$ for $n \geq 1$.

Theorem 2.1. *If A1 holds and the time-step size $\tau_n \leq \frac{4\epsilon^2(1+2r_n)}{\kappa(1+r_n)}$, the variable-steps BDF2 time-stepping scheme (1.7) is uniquely solvable.*

Proof. For any fixed time-level indexes $n \geq 2$, consider the following energy functional G on the space $\mathbb{V}_h^* := \{z \in \mathbb{V}_h \mid \langle z, 1 \rangle = \langle \phi^{n-1}, 1 \rangle\}$,

$$G[z] := \frac{1}{2} b_0^{(n)} \|z - \phi^{n-1}\|_{-1}^2 + b_1^{(n)} \langle \nabla_\tau \phi^{n-1}, z - \phi^{n-1} \rangle_{-1} + \frac{\kappa \epsilon^2}{2} \|\nabla_h z\|^2 + \kappa \langle F(z), 1 \rangle. \quad (2.4)$$

Under the time-step condition $\tau_n \leq \frac{4\epsilon^2(1+2r_n)}{\kappa(1+r_n)}$ or $b_0^{(n)} \epsilon^2 \geq \frac{\kappa}{4}$, the functional G is strictly convex since, for any $\lambda \in \mathbb{R}$ and any $\psi \in \mathring{\mathbb{V}}_h$,

$$\begin{aligned} \frac{d^2 G}{d\lambda^2} [z + \lambda \psi] \Big|_{\lambda=0} &= b_0^{(n)} \|\psi\|_{-1}^2 + \kappa \epsilon^2 \|\nabla_h \psi\|^2 + 3\kappa \|z\psi\|^2 - \kappa \|\psi\|^2 \\ &\geq \|\nabla_h \psi\| \|\psi\|_{-1} - \kappa \|\psi\|^2 + 3\kappa \|z\psi\|^2 > 0, \end{aligned}$$

where the generalized Hölder inequality (2.2) has been applied in the last step. Thus the functional G has a unique minimizer, denoted by ϕ^n , if and only if it solves the equation

$$\begin{aligned} 0 &= \frac{dG}{d\lambda} [z + \lambda \psi] \Big|_{\lambda=0} = \langle b_0^{(n)} (z - \phi^{n-1}) + b_1^{(n)} \nabla_\tau \phi^{n-1}, \psi \rangle_{-1} + \kappa \langle -\epsilon^2 \Delta_h z + F'(z), \psi \rangle \\ &= \left\langle b_0^{(n)} (z - \phi^{n-1}) + b_1^{(n)} \nabla_\tau \phi^{n-1} - \kappa \Delta_h (F'(z) - \epsilon^2 \Delta_h z), \psi \right\rangle_{-1}. \end{aligned}$$

This equation holds for any $\psi \in \mathring{\mathbb{V}}_h$ if and only if the unique minimizer $\phi^n \in \mathbb{V}_h^*$ solves

$$b_0^{(n)} (\phi^n - \phi^{n-1}) + b_1^{(n)} \nabla_\tau \phi^{n-1} - \kappa \Delta_h (F'(\phi^n) - \epsilon^2 \Delta_h \phi^n) = 0,$$

which is just the BDF2 scheme (1.7). It completes the proof. \square

The proof of Theorem 2.1 also says that the solution of the BDF2 scheme (1.7) is equivalent to the minimization of a convex functional $G[z]$ under the condition $\tau_n \leq \frac{4\epsilon^2(1+2r_n)}{\kappa(1+r_n)}$. We see that the BDF2 implicit scheme is also convex according to Xu et al. [29].

2.2 Discrete energy dissipation law

In our previous work [22, Lemma 2.1], the BDF2 kernels $b_{n-k}^{(n)}$ are shown to be positive definite if the adjacent time-step ratios $0 < r_k < \frac{3+\sqrt{17}}{2}$. The following result shows that this sufficient condition can be further improved in the theoretical manner. This improvement is inspired

by [18, LemmaA.1] to find a lower bound for the eigenvalues of the step-scaled matrix \tilde{B} , see Lemma 3.2 below. For simplicity, we denote

$$R_L(z, s) := \frac{2 + 4z - z^{3/2}}{1 + z} - \frac{s^{3/2}}{1 + s} \quad \text{for } 0 \leq z, s \leq r_*, \quad (2.5)$$

where $r_* \approx 4.864$ is the positive root of the equation $1 + 2r_* - r_*^{3/2} = 0$. According to the proof of [18, LemmaA.1], $R_L(z, s)$ is increasing in $(0, 1)$ and decreasing in $(1, r_*)$ with respect to z . Also, $R_L(z, s)$ is decreasing with respect to s such that

$$R_L(z, s) > \min\{R_L(0, r_*), R_L(r_*, r_*)\} = \frac{2(1 + 2r_* - r_*^{3/2})}{1 + z} = 0 \quad \text{for } 0 < z, s < r_*.$$

Lemma 2.1. *Let $0 < r_k < 4.864$ for $2 \leq k \leq N$. For any real sequence $\{w_k\}_{k=1}^n$ with n entries, it holds that*

$$2w_k \sum_{j=1}^k b_{k-j}^{(k)} w_j \geq \frac{r_{k+1}^{3/2}}{1 + r_{k+1}} \frac{w_k^2}{\tau_k} - \frac{r_k^{3/2}}{1 + r_k} \frac{w_{k-1}^2}{\tau_{k-1}} + R_L(r_k, r_{k+1}) \frac{w_k^2}{\tau_k} \quad \text{for } k \geq 2.$$

So the discrete convolution kernels $b_{n-k}^{(n)}$ are positive definite in the sense that

$$2 \sum_{k=2}^n w_k \sum_{j=2}^k b_{k-j}^{(k)} w_j \geq \sum_{k=2}^n R_L(r_k, r_{k+1}) \frac{w_k^2}{\tau_k} \quad \text{for } n \geq 2.$$

Proof. Applying the inequality $-2ab \geq -a^2 - b^2$, we take $u_k := w_k / \sqrt{\tau_k}$ to find

$$\begin{aligned} 2w_k \sum_{j=1}^k b_{k-j}^{(k)} w_j &= 2\tau_k b_0^{(k)} u_k^2 + 2\sqrt{\tau_k \tau_{k-1}} b_1^{(k)} u_k u_{k-1} \\ &\geq \frac{2 + 4r_k}{1 + r_k} u_k^2 - \frac{r_k^{3/2}}{1 + r_k} (u_k^2 + u_{k-1}^2) \\ &= \frac{r_{k+1}^{3/2}}{1 + r_{k+1}} \frac{w_k^2}{\tau_k} - \frac{r_k^{3/2}}{1 + r_k} \frac{w_{k-1}^2}{\tau_{k-1}} + R_L(r_k, r_{k+1}) \frac{w_k^2}{\tau_k} \quad \text{for } k \geq 2. \end{aligned}$$

Summing this inequality from $k = 2$ to n , it is straightforward to obtain the claimed second inequality and complete the proof. \square

Remark 2. *This lemma updates the sufficient condition of [22, Lemma 2.1]. Thus by following the discussions in [22, Remark 3 and Remark 5], one can verify that the variable-step BDF2 method is A-stable and zero-stable if the adjoint time-step ratios r_k satisfy the updated sufficient condition: $0 < r_k < 4.864$ for $2 \leq k \leq N$.*

Let $E[\phi^k]$ be the discrete version of free energy functional (1.1), given by

$$E[\phi^k] := \frac{\epsilon^2}{2} \|\nabla_h \phi^k\|^2 + \langle F(\phi^k), 1 \rangle \quad \text{for } k \geq 1. \quad (2.6)$$

Next theorem shows that the numerical scheme (1.7) preserves a modified energy dissipation property at the discrete levels, and it is mesh-robustly stable in an energy norm if **S0** holds.

Theorem 2.2. *Let $\mathbf{S0}$ holds. If the time-step sizes are properly small such that*

$$\tau_n \leq \frac{4\epsilon^2}{\kappa} \min \left\{ \frac{1+2r_n}{1+r_n}, R_L(r_n, r_{n+1}) \right\} \quad \text{for } n \geq 2, \quad (2.7)$$

the BDF2 scheme (1.7) preserves the following energy dissipation law

$$\mathcal{E}[\phi^n] \leq \mathcal{E}[\phi^{n-1}] \leq \mathcal{E}[\phi^1] \quad \text{for } n \geq 2,$$

where the modified discrete energy $\mathcal{E}[\phi^n]$ is defined by

$$\mathcal{E}[\phi^k] := E[\phi^k] + \frac{\sqrt{r_{k+1}\tau_{k+1}}}{2\kappa(1+r_{k+1})} \|\partial_\tau \phi^k\|_{-1}^2 \quad \text{for } k \geq 1. \quad (2.8)$$

Proof. The first condition of (2.7) ensures the unique solvability. We will establish the energy dissipation law under the second condition of (2.7). The volume conservation implies $\nabla_\tau \phi^n \in \mathbb{V}_h$ for $n \geq 1$. Then we make the inner product of (1.7) by $(-\Delta_h)^{-1} \nabla_\tau \phi^n / \kappa$ and obtain

$$\frac{1}{\kappa} \langle D_2 \phi^n, \nabla_\tau \phi^n \rangle_{-1} - \epsilon^2 \langle \Delta_h \phi^n, \nabla_\tau \phi^n \rangle + \langle F'(\phi^n), \nabla_\tau \phi^n \rangle = 0. \quad (2.9)$$

With the help of the summation by parts and $2a(a-b) = a^2 - b^2 + (a-b)^2$, the second term at the left hand side of (2.9) reads

$$\epsilon^2 \langle \nabla_h \phi^n, \nabla_\tau \nabla_h \phi^n \rangle = \frac{\epsilon^2}{2} \|\nabla_h \phi^n\|^2 - \frac{\epsilon^2}{2} \|\nabla_h \phi^{n-1}\|^2 + \frac{\epsilon^2}{2} \|\nabla_h \nabla_\tau \phi^n\|^2.$$

It is easy to check the following identity

$$4(a^3 - a)(a-b) = (a^2 - 1)^2 - (b^2 - 1)^2 - 2(a-b)^2 + 2a^2(a-b)^2 + (a^2 - b^2)^2.$$

Then the third term in (2.9) can be bounded by

$$\langle F'(\phi^n), \nabla_\tau \phi^n \rangle \geq \langle F(\phi^n), 1 \rangle - \langle F(\phi^{n-1}), 1 \rangle - \frac{1}{2} \|\nabla_\tau \phi^n\|^2.$$

Recalling the generalized Hölder inequality (2.2), one gets

$$\frac{1}{2} \|\nabla_\tau \phi^n\|^2 \leq \frac{1}{2} \|\nabla_h \nabla_\tau \phi^n\| \|\nabla_\tau \phi^n\|_{-1} \leq \frac{\epsilon^2}{2} \|\nabla_h \nabla_\tau \phi^n\|^2 + \frac{1}{8\epsilon^2} \|\nabla_\tau \phi^n\|_{-1}^2.$$

Thus it follows from (2.9) that

$$\frac{1}{\kappa} \langle D_2 \phi^n, \nabla_\tau \phi^n \rangle_{-1} - \frac{1}{8\epsilon^2} \|\nabla_\tau \phi^n\|_{-1}^2 + E[\phi^n] \leq E[\phi^{n-1}] \quad \text{for } n \geq 2. \quad (2.10)$$

The second condition of (2.7) gives $R_L(r_n, r_{n+1}) \geq \kappa\tau_n/(4\epsilon^2)$. Taking $w_j = \nabla_\tau \phi^j$ in the first inequality of Lemma 2.1, it is not difficult to get

$$\frac{1}{\kappa} \langle D_2 \phi^n, \nabla_\tau \phi^n \rangle_{-1} \geq \frac{\sqrt{r_{n+1}\tau_{n+1}}}{2\kappa(1+r_{n+1})} \|\partial_\tau \phi^n\|_{-1}^2 - \frac{\sqrt{r_n\tau_n}}{2\kappa(1+r_n)} \|\partial_\tau \phi^{n-1}\|_{-1}^2 + \frac{1}{8\epsilon^2} \|\nabla_\tau \phi^n\|_{-1}^2.$$

Combining it with (2.10) yields $\mathcal{E}[\phi^n] \leq \mathcal{E}[\phi^{n-1}]$ for $n \geq 2$. It completes the proof. \square

Remark 3. It is seen that this time-step constraint (2.7) requires $\tau_n = O(\epsilon^2/\kappa)$ and is essentially determined by the interface width parameter ϵ . In practical simulations, this condition is acceptable since $\tau_n = O(\epsilon^2/\kappa)$ is always necessary in the L^2 norm stability or convergence analysis, cf. [7–9, 29].

Lemma 2.2. Let **S0** and **A1** hold. If the step sizes τ_n fulfill (2.7), the solution of BDF2 implicit time-stepping scheme (1.7) is bounded in the sense that

$$\|\phi^n\| + \|\nabla_h \phi^n\| \leq c_1 := \sqrt{4\epsilon^{-2}c_0 + (2 + \epsilon^2)|\Omega_h|} \quad \text{for } n \geq 2,$$

where c_1 is dependent on the domain Ω , the interface parameter ϵ and the starting value ϕ^1 , but independent of the time t_n , the time-step sizes τ_n and the time-step ratios r_n .

Proof. Under the assumption **A1**, the definition (2.8) of $\mathcal{E}[\phi^n]$ gives

$$\mathcal{E}[\phi^1] \leq E[\phi^1] + \frac{\tau_2}{2\kappa} \|\partial_\tau \phi^1\|_{-1}^2 \leq c_0$$

Thus the discrete energy dissipation law in Theorem 2.2 implies $c_0 \geq \mathcal{E}[\phi^n] \geq E[\phi^n]$. Reminding the inequality $\|\phi^n\|_{l^4}^4 \geq 2(1 + \epsilon^2)\|\phi^n\|^2 - (1 + \epsilon^2)^2|\Omega_h|$, due to the simple fact $(a^2 - 1 - \epsilon^2)^2 \geq 0$, one applies the definition (2.6) of $E[\phi^n]$ to get

$$4c_0 \geq 2\epsilon^2\|\nabla_h \phi^n\|^2 + 4\langle F(\phi^n), 1 \rangle \geq 2\epsilon^2\|\nabla_h \phi^n\|^2 + 2\epsilon^2\|\phi^n\|^2 - \epsilon^2(2 + \epsilon^2)|\Omega_h|,$$

and then

$$(\|\phi^n\| + \|\nabla_h \phi^n\|)^2 \leq 2\|\phi^n\|^2 + 2\|\nabla_h \phi^n\|^2 \leq 4\epsilon^{-2}c_0 + (2 + \epsilon^2)|\Omega_h| \quad \text{for } n \geq 2.$$

It implies the claimed result and completes the proof. \square

3 Some discrete convolution inequalities

Our error analysis is closely related to the convolution form (1.11), so we need some detail properties and discrete convolution inequalities with respect to the DOC kernels $\theta_{n-j}^{(n)}$. It is to emphasize that the positive constants \mathbf{m}_1 , \mathbf{m}_2 and \mathbf{m}_3 involved in this section are independent of the time t_n , time-step sizes τ_n and the step ratios r_n . Actually, they would take different values for different choices of step ratios r_n , but are bounded with respect to the changes of step ratios, even when r_n approaches the user limit r_{user} .

3.1 Simple properties of DOC kernels

Following the proofs of [22, Lemma 2.2, Corollary 2.1 and Lemma 2.3], we can obtain some simple properties of the DOC kernels.

Lemma 3.1. If **S0** holds, the DOC kernels $\theta_{n-j}^{(n)}$ defined in (1.8) satisfy:

(I) The discrete kernels $\theta_{n-j}^{(n)}$ are positive definite;

(II) The discrete kernels $\theta_{n-j}^{(n)}$ are positive and $\theta_{n-j}^{(n)} = \frac{1}{b_0^{(j)}} \prod_{i=j+1}^n \frac{r_i^2}{1 + 2r_i}$ for $2 \leq j \leq n$;

$$(III) \sum_{j=2}^n \theta_{n-j}^{(n)} \leq \tau_n \text{ such that } \sum_{k=2}^n \sum_{j=2}^k \theta_{k-j}^{(k)} \leq t_n \text{ for } n \geq 2.$$

We introduce the following two $(n-1) \times (n-1)$ matrices

$$B_2 := \begin{pmatrix} b_0^{(2)} & & & \\ b_1^{(3)} & b_0^{(3)} & & \\ & \ddots & \ddots & \\ & & b_1^{(n)} & b_0^{(n)} \end{pmatrix} \quad \text{and} \quad \Theta_2 := \begin{pmatrix} \theta_0^{(2)} & & & \\ \theta_1^{(3)} & \theta_0^{(3)} & & \\ \vdots & \vdots & \ddots & \\ \theta_{n-2}^{(n)} & \theta_{n-3}^{(n)} & \cdots & \theta_0^{(n)} \end{pmatrix},$$

where the discrete kernels $b_{n-k}^{(n)}$ and $\theta_{n-k}^{(n)}$ are defined by (1.6) and (1.8), respectively. It follows from the discrete orthogonal identity (1.9) that

$$\Theta_2 = B_2^{-1}. \quad (3.1)$$

If the step ratios condition **S0** holds, Lemma 2.1 shows that the real symmetric matrix

$$B := B_2 + B_2^T \quad (3.2)$$

is positive definite, that is,

$$\mathbf{w}^T B \mathbf{w} = 2 \sum_{k=2}^n w^k \sum_{j=2}^k b_{k-j}^{(k)} w^j \geq \sum_{k=1}^n \frac{R_L(r_k, r_{k+1})}{\tau_k} (w^k)^2,$$

where the function $R_L(z, s)$ is defined by (2.5) and the vector $\mathbf{w} := (w^2, w^3, \dots, w^n)^T$. According to Lemma 3.1 (I), the following symmetric matrix

$$\Theta := \Theta_2 + \Theta_2^T = B_2^{-1} + (B_2^{-1})^T = (B_2^{-1})^T (B_2 + B_2^T) B_2^{-1} = (B_2^{-1})^T B B_2^{-1} \quad (3.3)$$

is also positive definite in the sense of $\mathbf{w}^T \Theta \mathbf{w} = 2 \sum_{k,j}^{n,k} \theta_{k-j}^{(k)} w^j w^k > 0$. Here and hereafter, we denote $\sum_{k,j}^{n,k} := \sum_{k=2}^n \sum_{j=2}^k$ for the simplicity of presentation.

3.2 Eigenvalue estimates

To facilitate the proofs in what follows, we are to define the following step-scaled matrix

$$\tilde{B}_2 := \Lambda_\tau B_2 \Lambda_\tau = \begin{pmatrix} \tilde{b}_0^{(2)} & & & \\ \tilde{b}_1^{(3)} & \tilde{b}_0^{(3)} & & \\ & \ddots & \ddots & \\ & & \tilde{b}_1^{(n)} & \tilde{b}_0^{(n)} \end{pmatrix}_{(n-1) \times (n-1)}, \quad (3.4)$$

where the diagonal matrix $\Lambda_\tau := \text{diag}(\sqrt{\tau_2}, \sqrt{\tau_3}, \dots, \sqrt{\tau_n})$ so that the step-scaled discrete kernels $\tilde{b}_0^{(k)}$ and $\tilde{b}_1^{(k)}$ are given by

$$\tilde{b}_0^{(k)} = \frac{1 + 2r_k}{1 + r_k} \quad \text{and} \quad \tilde{b}_1^{(k)} = -\frac{r_k^{3/2}}{1 + r_k} \quad \text{for } 2 \leq k \leq n. \quad (3.5)$$

Moreover, we will use the following real symmetric matrix,

$$\tilde{B} := \tilde{B}_2 + \tilde{B}_2^T = \Lambda_\tau B \Lambda_\tau. \quad (3.6)$$

The following two lemmas present some eigenvalue estimates of \tilde{B} and $\tilde{B}_2^T \tilde{B}_2$. To avoid possible confusions, we define the vector norm $\|\cdot\|$ by $\|\mathbf{u}\| := \sqrt{\mathbf{u}^T \mathbf{u}}$ for any real vector \mathbf{u} and the associated matrix norm $\|A\| := \sqrt{\lambda_{\max}(A^T A)}$.

Lemma 3.2. *If S0 holds, there exists a positive constant \mathfrak{m}_1 such that $\lambda_{\min}(\tilde{B}) \geq \mathfrak{m}_1 > 0$.*

Proof. This proof can be followed from [18, Lemma A.1]. We include the main ingredient for the completeness. Applying the Gerschgorin's circle theorem to the matrix \tilde{B} , one has

$$\lambda_{\min}(\tilde{B}) \geq \min_{2 \leq k \leq n} R_L(r_k, r_{k+1}) > R_L(r_{\text{user}}, r_{\text{user}}) = \frac{2(1 + 2r_{\text{user}} - r_{\text{user}}^{3/2})}{1 + r_{\text{user}}} > 0,$$

where $R_L(z, s)$ is defined by (2.5). It completes the proof by taking $\mathfrak{m}_1 = \frac{2(1+2r_{\text{user}}-r_{\text{user}}^{3/2})}{1+r_{\text{user}}}$. \square

Lemma 3.3. *If S0 holds, there exists a positive constant \mathfrak{m}_2 such that $\lambda_{\max}(\tilde{B}_2^T \tilde{B}_2) \leq \mathfrak{m}_2$.*

Proof. This proof can be followed from [18, Lemma A.2]. We include the main ingredient for the completeness. By writing out the tri-diagonal matrix $\tilde{B}_2^T \tilde{B}_2$ and applying the Gerschgorin's circle theorem, one can find

$$\lambda_{\max}(\tilde{B}_2^T \tilde{B}_2) \leq \max_{2 \leq k \leq n} R_U(r_k, r_{k+1}) < R_U(r_{\text{user}}, r_{\text{user}}),$$

where the function $R_U(z, s)$ is defined by

$$R_U(z, s) := \frac{(1+2z)(1+2z+z^{3/2})}{(1+z)^2} + \frac{s^{3/2}(1+2s+s^{3/2})}{(1+s)^2} \quad \text{for } 0 \leq z, s < r_{\text{user}}.$$

An upper bound is then obtained by taking $\mathfrak{m}_2 = R_U(r_{\text{user}}, r_{\text{user}})$. \square

By the above two lemmas, we can bound the minimum eigenvalue of Θ .

Lemma 3.4. *If S0 holds, the real symmetric matrix Θ in (3.3) satisfies*

$$\mathbf{v}^T \Theta \mathbf{v} \geq \frac{\mathfrak{m}_1}{\mathfrak{m}_2} \|\Lambda_\tau \mathbf{v}\|^2 \quad \text{for any vector } \mathbf{v}.$$

Proof. Lemma 3.2 says that real symmetric matrix \tilde{B} is positive definite. There exists a non-singular upper triangular matrix \tilde{U} such that $\tilde{B} = \tilde{U}^T \tilde{U}$. By using (3.3) and (3.6), one gets

$$\mathbf{v}^T \Theta \mathbf{v} = \mathbf{v}^T (B_2^{-1})^T B B_2^{-1} \mathbf{v} = \mathbf{v}^T (B_2^{-1})^T \Lambda_\tau^{-1} \tilde{B} \Lambda_\tau^{-1} B_2^{-1} \mathbf{v} = \|\tilde{U} \Lambda_\tau^{-1} B_2^{-1} \mathbf{v}\|^2.$$

Thus it follows that

$$\begin{aligned} \|\Lambda_\tau \mathbf{v}\|^2 &= \|\Lambda_\tau B_2 \Lambda_\tau \tilde{U}^{-1} \tilde{U} \Lambda_\tau^{-1} B_2^{-1} \mathbf{v}\|^2 \leq \|\tilde{B}_2 \tilde{U}^{-1}\|^2 \|\tilde{U} \Lambda_\tau^{-1} B_2^{-1} \mathbf{v}\|^2 \\ &\leq \|\tilde{B}_2\|^2 \|\tilde{U}^{-1}\|^2 \mathbf{v}^T \Theta \mathbf{v} = \lambda_{\max}(\tilde{B}_2^T \tilde{B}_2) \lambda_{\max}(\tilde{B}^{-1}) \mathbf{v}^T \Theta \mathbf{v}. \end{aligned}$$

Thus Lemmas 3.2 and 3.3 yield the claimed inequality. \square

To evaluate the maximum eigenvalue of Θ , consider the inverse matrix of the matrix \tilde{B}_2 ,

$$\tilde{\Theta}_2 := \tilde{B}_2^{-1} = \Lambda_\tau^{-1} \Theta_2 \Lambda_\tau^{-1} = \begin{pmatrix} \tilde{\theta}_0^{(2)} & & & \\ \tilde{\theta}_1^{(3)} & \tilde{\theta}_0^{(3)} & & \\ \vdots & \vdots & \ddots & \\ \tilde{\theta}_{n-2}^{(n)} & \tilde{\theta}_{n-3}^{(n)} & \cdots & \tilde{\theta}_0^{(n)} \end{pmatrix}, \quad (3.7)$$

where the step-scaled DOC kernels $\tilde{\theta}_{k-j}^{(k)}$ follow from Lemma 3.1 (II),

$$\tilde{\theta}_{k-j}^{(k)} := \frac{1}{\sqrt{\tau_k \tau_j}} \theta_{k-j}^{(k)} = \frac{1+r_j}{1+2r_j} \prod_{i=j+1}^k \frac{r_i^{3/2}}{1+2r_i} \quad \text{for } 2 \leq j \leq k \leq n. \quad (3.8)$$

Lemma 3.5. *If S0 holds, then there exists a positive constant \mathfrak{m}_3 such that*

$$\mathbf{v}^T \Theta \mathbf{v} \leq \mathfrak{m}_3 \|\Lambda_\tau \mathbf{v}\|^2 \quad \text{for any vector } \mathbf{v}.$$

Proof. Let $\tilde{\Theta} = \tilde{\Theta}_2 + \tilde{\Theta}_2^T$. Since $0 < \frac{x^{3/2}}{1+2x} < m_* := \frac{r_{\text{user}}^{3/2}}{1+2r_{\text{user}}} < 1$ any $x \in [0, r_{\text{user}}]$, one can apply the formula (3.8) to get

$$\mathfrak{R}_{n,k} := \sum_{j=2}^k \tilde{\theta}_{k-j}^{(k)} + \sum_{j=k}^n \tilde{\theta}_{j-k}^{(j)} \leq \sum_{j=2}^k m_*^{k-j} + \sum_{j=k}^n m_*^{j-k} < \frac{2}{1-m_*} \quad \text{for } 2 \leq k \leq n.$$

One has $\lambda_{\max}(\tilde{\Theta}) \leq \max_{2 \leq k \leq n} \mathfrak{R}_{n,k} < \mathfrak{m}_3 := \frac{2}{1-m_*}$ by the Gerschgorin's circle theorem. It implies $\mathbf{w}^T \tilde{\Theta} \mathbf{w} \leq \mathfrak{m}_3 \|\mathbf{w}\|^2$ for any \mathbf{w} and the choice $\mathbf{w} := \Lambda_\tau \mathbf{v}$ completes the proof. \square

3.3 Discrete convolution inequalities

The following two lemmas describe the Young-type convolution inequality.

Lemma 3.6. *If S0 holds, then for any real sequences $\{v^k\}_{k=2}^n$ and $\{w^k\}_{k=2}^n$,*

$$\sum_{k,j}^{n,k} \theta_{k-j}^{(k)} w^k v^j \leq \varepsilon \sum_{k,j}^{n,k} \theta_{k-j}^{(k)} v^k v^j + \frac{1}{2\mathfrak{m}_1 \varepsilon} \sum_{k=2}^n \tau_k (w^k)^2 \quad \text{for } \forall \varepsilon > 0.$$

Proof. Let $\mathbf{w} := (w^2, w^3, \dots, w^n)^T$. A similar proof of [18, Lemma A.3] gives

$$\sum_{k,j}^{n,k} \theta_{k-j}^{(k)} v^j w^k \leq \varepsilon \sum_{k,j}^{n,k} \theta_{k-j}^{(k)} v^j v^k + \frac{1}{2\varepsilon} \mathbf{w}^T B^{-1} \mathbf{w} \quad \text{for any } \varepsilon > 0.$$

From the proof Lemma 3.4, we have $B^{-1} = \Lambda_\tau \tilde{U}^{-1} (\Lambda_\tau \tilde{U}^{-1})^T$ and then

$$\begin{aligned} \mathbf{w}^T B^{-1} \mathbf{w} &= \mathbf{w}^T \Lambda_\tau \tilde{U}^{-1} (\Lambda_\tau \tilde{U}^{-1})^T \mathbf{w} = \|\tilde{U}^{-1})^T \Lambda_\tau \mathbf{w}\|^2 \\ &\leq \|\tilde{U}^{-1})^T\|^2 \|\Lambda_\tau \mathbf{w}\|^2 = \lambda_{\max}((\tilde{B})^{-1}) \mathbf{w}^T \Lambda_\tau^2 \mathbf{w} \leq \mathfrak{m}_1^{-1} \sum_{k=2}^n \tau_k (w^k)^2, \end{aligned}$$

where Lemma 3.2 has been used. It completes the proof. \square

Lemma 3.7. *If **S0** holds, then for any real sequences $\{v^k\}_{k=2}^n$ and $\{w^k\}_{k=2}^n$,*

$$\sum_{k,j}^{n,k} \theta_{k-j}^{(k)} w^k v^j \leq \varepsilon \sum_{k=2}^n \tau_k (v^k)^2 + \frac{\mathfrak{m}_3}{4\mathfrak{m}_1 \varepsilon} \sum_{k=2}^n \tau_k (w^k)^2 \quad \text{for } \forall \varepsilon > 0.$$

Proof. For fixed time index n , taking $\varepsilon := 2\varepsilon_0/\mathfrak{m}_3$ in Lemma 3.6 yields

$$\begin{aligned} \sum_{k,j}^{n,k} \theta_{k-j}^{(k)} w^k v^j &\leq \frac{2\varepsilon_0}{\mathfrak{m}_3} \sum_{k,j}^{n,k} \theta_{k-j}^{(k)} v^k v^j + \frac{\mathfrak{m}_3}{4\mathfrak{m}_1 \varepsilon_0} \sum_{k=2}^n \tau_k (w^k)^2 \\ &\leq \varepsilon_0 \sum_{k=2}^n \tau_k (v^k)^2 + \frac{\mathfrak{m}_3}{4\mathfrak{m}_1 \varepsilon_0} \sum_{k=2}^n \tau_k (w^k)^2, \end{aligned}$$

where Lemma 3.5 was used in the last inequality. It completes the proof by choosing $\varepsilon_0 := \varepsilon$. \square

We now present two discrete embedding-type convolution inequalities by considering three time-space discrete functions u^k , v^k and w^k ($1 \leq k \leq n$) in the space \mathbb{V}_h or its subspace $\mathring{\mathbb{V}}_h$.

Lemma 3.8. *Assume that $u^k, w^k \in \mathbb{V}_h$, $v^k \in \mathring{\mathbb{V}}_h$ ($2 \leq k \leq n$) and there exists a constant c_u such that $\|u^k\|_{l^3} \leq c_u$ for $2 \leq k \leq n$. If **S0** holds, then for any $\varepsilon > 0$,*

$$\sum_{k,j}^{n,k} \theta_{k-j}^{(k)} \langle u^j v^j, w^k \rangle \leq \varepsilon \sum_{k,j}^{n,k} \theta_{k-j}^{(k)} \langle \nabla_h v^j, \nabla_h v^k \rangle + \frac{c_z^2 c_u^2 \mathfrak{m}_2 \mathfrak{m}_3}{2\mathfrak{m}_1^2 \varepsilon} \sum_{k=2}^n \tau_k \|w^k\|^2.$$

Proof. For fixed time index n , taking $v^j := u_h^j v_h^j$ and $\varepsilon := \varepsilon_1$ in Lemma 3.7, we have

$$\sum_{k,j}^{n,k} \theta_{k-j}^{(k)} \langle u^j v^j, w^k \rangle \leq \varepsilon_1 \sum_{k=2}^n \tau_k \|u^k v^k\|^2 + \frac{\mathfrak{m}_3}{4\mathfrak{m}_1 \varepsilon_1} \sum_{k=2}^n \tau_k \|w^k\|^2.$$

The well-known Hölder inequality and the discrete embedding inequality (2.3) imply that $\|u^k v^k\| \leq \|u^k\|_{l^3} \|v^k\|_{l^6} \leq c_z \|u^k\|_{l^3} \|\nabla_h v^k\| \leq c_z c_u \|\nabla_h v^k\|$. We derive that

$$\sum_{k=2}^n \tau_k \|u^k v^k\|^2 \leq c_z^2 c_u^2 \sum_{k=2}^n \tau_k \|\nabla_h v^k\|^2.$$

Then it follows that

$$\sum_{k,j}^{n,k} \theta_{k-j}^{(k)} \langle u^j v^j, w^k \rangle \leq \varepsilon_1 c_z^2 c_u^2 \sum_{k=2}^n \tau_k \|\nabla_h v^k\|^2 + \frac{\mathfrak{m}_3}{4\mathfrak{m}_1 \varepsilon_1} \sum_{k=2}^n \tau_k \|w^k\|^2. \quad (3.9)$$

Following the proof of Lemma 3.4, it is not difficult to get (cf. [19])

$$\sum_{k=2}^n \tau_k \|\nabla_h v^k\|^2 \leq \frac{2\mathfrak{m}_2}{\mathfrak{m}_1} \sum_{k,j}^{n,k} \theta_{k-j}^{(k)} \langle \nabla_h v^j, \nabla_h v^k \rangle.$$

Inserting this inequality into (3.9) and choosing the parameter $\varepsilon_1 := \mathfrak{m}_1 \varepsilon / (2c_z^2 c_u^2 \mathfrak{m}_2)$, we get the claimed inequality and complete the proof. \square

Lemma 3.9. Assume that $u^k \in \mathbb{V}_h$, $w^k \in \mathring{\mathbb{V}}_h$ ($2 \leq k \leq n$) and there exists a constant c_u such that $\|u^k\|_{l^3} \leq c_u$ for $2 \leq k \leq n$. If **S0** holds, then for any $\varepsilon > 0$,

$$\sum_{k,j}^{n,k} \theta_{k-j}^{(k)} \langle u^j w^j, \Delta_h w^k \rangle \leq \varepsilon \sum_{k,j}^{n,k} \theta_{k-j}^{(k)} \langle \Delta_h w^j, \Delta_h w^k \rangle + \frac{c_z^4 c_u^4 \mathfrak{m}_2^3 \mathfrak{m}_3^2}{\mathfrak{m}_1^5 \varepsilon^3} \sum_{k=2}^n \tau_k \|w^k\|^2.$$

Proof. For fixed time index n , we start the proof from (3.9) by setting $w^j := \Delta_h w^j$, $v^j := w^j$ and $\varepsilon_1 := \mathfrak{m}_2 \mathfrak{m}_3 / (\varepsilon_4 \mathfrak{m}_1^2)$, that is,

$$\begin{aligned} \sum_{k,j}^{n,k} \theta_{k-j}^{(k)} \langle u^j w^j, \Delta_h w^k \rangle &\leq \frac{c_z^2 c_u^2 \mathfrak{m}_2 \mathfrak{m}_3}{2 \mathfrak{m}_1^2 \varepsilon_4} \sum_{k=2}^n \tau_k \|\nabla_h w^k\|^2 + \frac{\mathfrak{m}_1 \varepsilon_4}{2 \mathfrak{m}_2} \sum_{k=2}^n \tau_k \|\Delta_h w^k\|^2 \\ &\leq \frac{c_z^2 c_u^2 \mathfrak{m}_2 \mathfrak{m}_3}{2 \mathfrak{m}_1^2 \varepsilon_4} \sum_{k=2}^n \tau_k \|\nabla_h w^k\|^2 + \varepsilon_4 \sum_{k,j}^{n,k} \theta_{k-j}^{(k)} \langle \Delta_h w^j, \Delta_h w^k \rangle, \end{aligned} \quad (3.10)$$

where Lemma 3.4 has been used to handle the last term. Furthermore, by using the classical Young's inequality and Lemma 3.4, one gets

$$\begin{aligned} \sum_{k=2}^n \tau_k \|\nabla_h w^k\|^2 &= \sum_{k=2}^n \tau_k \langle -\Delta_h w^k, w^k \rangle \leq \frac{\varepsilon_3}{2} \sum_{k=2}^n \tau_k \|\Delta_h w^k\|^2 + \frac{1}{2\varepsilon_3} \sum_{k=2}^n \tau_k \|w^k\|^2 \\ &\leq \frac{\mathfrak{m}_2 \varepsilon_3}{\mathfrak{m}_1} \sum_{k,j}^{n,k} \theta_{k-j}^{(k)} \langle \Delta_h w^j, \Delta_h w^k \rangle + \frac{1}{2\varepsilon_3} \sum_{k=2}^n \tau_k \|w^k\|^2. \end{aligned}$$

Inserting this inequality into (3.10), we have

$$\begin{aligned} \sum_{k,j}^{n,k} \theta_{k-j}^{(k)} \langle u^j w^j, \Delta_h w^k \rangle &\leq \left(\frac{c_z^2 c_u^2 \mathfrak{m}_2^2 \mathfrak{m}_3 \varepsilon_3}{2 \mathfrak{m}_1^3 \varepsilon_4} + \varepsilon_4 \right) \sum_{k,j}^{n,k} \theta_{k-j}^{(k)} \langle \Delta_h w^j, \Delta_h w^k \rangle \\ &\quad + \frac{c_z^2 c_u^2 \mathfrak{m}_2 \mathfrak{m}_3}{4 \mathfrak{m}_1^2 \varepsilon_3 \varepsilon_4} \sum_{k=2}^n \tau_k \|w^k\|^2. \end{aligned}$$

Now by choosing $\varepsilon_4 := \varepsilon/2$ and $\varepsilon_3 := \mathfrak{m}_1^3 \varepsilon_4 \varepsilon / (c_z^2 c_u^2 \mathfrak{m}_2^2 \mathfrak{m}_3)$, we obtain the claimed inequality. \square

4 Robust L^2 norm error estimate

4.1 Convolutional consistency and technical lemma

Let $\xi_\Phi^j := D_2 \Phi(t_j) - \partial_t \Phi(t_j)$ be the local consistency error of BDF2 formula at the time $t = t_j$. We will consider a convolutional consistency error Ξ_Φ^k defined by

$$\Xi_\Phi^k := \sum_{j=2}^k \theta_{k-j}^{(k)} \xi_\Phi^j = \sum_{j=2}^k \theta_{k-j}^{(k)} (D_2 \Phi(t_j) - \partial_t \Phi(t_j)) \quad \text{for } k \geq 2. \quad (4.1)$$

By following the proof of [18, Lemma 3.4], one has

$$|\Xi_\Phi^k| \leq 3 \sum_{j=1}^k \theta_{k-j}^{(k)} \tau_j \int_{t_{j-1}}^{t_j} |\Phi'''(s)| \, ds \quad \text{for } k \geq 2.$$

Then Lemma 3.1 (III) yields the following estimate on the convolutional consistency.

Lemma 4.1. *If **S0** holds, the convolutional consistency error Ξ_Φ^k in (4.1) satisfies*

$$\sum_{k=2}^n |\Xi_\Phi^k| \leq 3t_n \max_{1 \leq j \leq n} \left(\tau_j \int_{t_{j-1}}^{t_j} |\Phi'''(s)| ds \right) \quad \text{for } n \geq 2.$$

We use the standard seminorms and norms in the Sobolev space $H^m(\Omega)$ for $m \geq 0$. Let $C_{per}^\infty(\Omega)$ be a set of infinitely differentiable L -periodic functions defined on Ω , and $H_{per}^m(\Omega)$ be the closure of $C_{per}^\infty(\Omega)$ in $H^m(\Omega)$, endowed with the semi-norm $|\cdot|_{H_{per}^m}$ and the norm $\|\cdot\|_{H_{per}^m}$.

For simplicity, denote $|\cdot|_{H^m} := |\cdot|_{H_{per}^m}$, $\|\cdot\|_{H^m} := \|\cdot\|_{H_{per}^m}$, and $\|\cdot\|_{L^2} := \|\cdot\|_{H^0}$. Next lemma lists some approximations, cf. [25, 26], of the L^2 -projection operator P_M and trigonometric interpolation operator I_M defined in subsection 2.1.

Lemma 4.2. *For any $u \in H_{per}^q(\Omega)$ and $0 \leq s \leq q$, it holds that*

$$\|P_M u - u\|_{H^s} \leq C_u h^{q-s} |u|_{H^q}, \quad \|P_M u\|_{H^s} \leq C_u \|u\|_{H^s}; \quad (4.2)$$

and, in addition if $q > 3/2$,

$$\|I_M u - u\|_{H^s} \leq C_u h^{q-s} |u|_{H^q}, \quad \|I_M u\|_{H^s} \leq C_u \|u\|_{H^s}. \quad (4.3)$$

4.2 Convergence analysis

Note that, the energy dissipation law (1.4) of CH model (1.2) shows that $E[\Phi^n] \leq E[\Phi(t_0)]$. From the formulation (1.1), it is easy to check that $\|\Phi^n\|_{H^1}$ can be bounded by a time-independent constant. Let $\Phi_M^n := (P_M \Phi)(\cdot, t_n)$ be the L^2 -projection of exact solution at time $t = t_n$. The projection estimate (4.2) in Lemma 4.2 yields

$$\|\Phi_M^n\| + \|\nabla_h \Phi_M^n\| \leq \|P_M \Phi^n\|_{H^1} \leq c_2 \quad \text{for } 1 \leq n \leq N, \quad (4.4)$$

where c_2 is dependent on the domain Ω and initial data $\Phi(t_0)$, but independent of the time t_n . We are in the position to prove the L^2 norm convergence of the adaptive BDF2 scheme (1.7).

Theorem 4.1. *Assume that the CH problem (1.2) has a solution $\Phi \in C^3([0, T]; H_{per}^{m+4})$ for some integer $m \geq 0$. Suppose further that the step-ratios condition **S0** and the time-step size constraint (2.7) hold such that the BDF2 scheme (1.7) is unique solvable and energy stable. If the maximum step size $\tau \leq 1/c_\epsilon$, the solution ϕ^n is robustly convergent in the L^2 norm,*

$$\begin{aligned} \|\Phi^n - \phi^n\| \leq C_\phi \exp(c_\epsilon t_{n-1}) & \left(\|\Phi_M^1 - \phi^1\| + \tau \|\partial_\tau(\Phi_M^1 - \phi^1)\| \right. \\ & \left. + t_n h^m + t_n \tau^2 \max_{0 < t \leq T} \|\Phi'''(t)\|_{L^2} \right) \quad \text{for } 2 \leq n \leq N, \end{aligned}$$

where $c_\epsilon := 4\kappa c_z^4 c_3^4 m_2^3 m_3^2 / (m_1^5 \epsilon^6)$ and $c_3 := c_\Omega^2 (c_1^2 + c_1 c_2 + c_2^2) + |\Omega_h|^{1/3}$ may be dependent on the given data, the solution and the starting values, but are always independent of the time t_n , time-step sizes τ_n and step ratios r_n . Specially, C_ϕ and c_ϵ remain bounded even when the step ratios r_n approach the user limit $r_{\text{user}} < 4.864$.

Proof. We evaluate the L^2 norm error $\|\Phi^n - \phi^n\|$ by a usual splitting,

$$\Phi^n - \phi^n = \Phi^n - \Phi_M^n + e^n,$$

where $e^n := \Phi_M^n - \phi^n \in \mathring{\mathbb{V}}_h$ is the difference between the projection Φ_M^n and the numerical solution ϕ^n of the BDF2 implicit scheme (1.7). Actually, the projection solution $\Phi_M^n \in \mathcal{F}_M$, the volume conservative property becomes available at the discrete level

$$\langle \Phi_M^n, 1 \rangle = \langle \Phi_M^0, 1 \rangle = \langle \phi^0, 1 \rangle = \langle \phi^n, 1 \rangle,$$

which implies the error function $e^n \in \mathring{\mathbb{V}}_h$. Applying Lemma 4.2, one has

$$\|\Phi^n - \Phi_M^n\| = \|I_M(\Phi^n - \Phi_M^n)\|_{L^2} \leq C_\phi \|I_M \Phi^n - \Phi_M^n\|_{L^2} \leq C_\phi h^m |\Phi^n|_{H^m}.$$

Once an upper bound of $\|e^n\|$ is available, the claimed error estimate follows immediately,

$$\|\Phi^n - \phi^n\| \leq \|\Phi^n - \Phi_M^n\| + \|e^n\| \leq C_\phi h^m |\Phi^n|_{H^m} + \|e^n\| \quad \text{for } 1 \leq n \leq N. \quad (4.5)$$

To bound $\|e^n\|$, we consider two stages: Stage 1 analyzes the space consistency error for a semi-discrete system having a projected solution Φ_M ; With the help of the Young-type and embedding convolution inequalities with respect to DOC kernels $\theta_{k-j}^{(k)}$ and the solution estimate in Lemma 2.2, Stage 2 derives the error estimate for the fully discrete error system.

Stage 1: Consistency analysis of semi-discrete projection A substitution of the projection solution Φ_M and differentiation operator Δ_h into the original equation (1.2) yields the semi-discrete system

$$\partial_t \Phi_M = \kappa \Delta_h \mu_M + \zeta_P \quad \text{with} \quad \mu_M = F'(\Phi_M) - \epsilon^2 \Delta_h \Phi_M, \quad (4.6)$$

where $\zeta_P(\mathbf{x}_h, t)$ represents the spatial consistency error arising from the projection of exact solution, that is,

$$\zeta_P := \partial_t \Phi_M - \partial_t \Phi + \kappa(\Delta \mu - \Delta_h \mu_M) \quad \text{for } \mathbf{x}_h \in \Omega_h. \quad (4.7)$$

Following the proof of [18, Theorem 3.1], and using Lemma 4.2, it is not difficult to obtain that $\|\zeta_P\| \leq C_\phi h^m$ and $\|\zeta_P(t_j)\| \leq C_\phi h^m$ for $j \geq 2$. Then Lemma 3.1 (III) yields

$$\sum_{k=2}^n \|\Upsilon_P^k\| \leq C_\phi h^m \sum_{k=2}^n \sum_{j=2}^k \theta_{k-j}^{(k)} \leq C_\phi t_n h^m \quad \text{where} \quad \Upsilon_P^k := \sum_{j=2}^k \theta_{k-j}^{(k)} \zeta_P(t_j) \quad \text{for } k \geq 2. \quad (4.8)$$

Stage 2: L^2 norm error of fully discrete system From the projection equation (4.6), one can apply the BDF2 formula to obtain the following approximation equation

$$D_2 \Phi_M^n = \kappa \Delta_h \mu_M^n + \zeta_P^n + \xi_\Phi^n \quad \text{with} \quad \mu_M^n = F'(\Phi_M^n) - \epsilon^2 \Delta_h \Phi_M^n, \quad (4.9)$$

where ξ_Φ^n is the local consistency error of BDF2 formula and $\zeta_P^n := \zeta_P(t_n)$ is defined by (4.7). Subtracting the full discrete scheme (1.7) from the approximation equation (4.9), we have the following error system

$$D_2 e^n = \kappa \Delta_h (-\epsilon^2 \Delta_h e^n + f_\phi^n e^n) + \zeta_P^n + \xi_\Phi^n \quad \text{for } 2 \leq n \leq N, \quad (4.10)$$

where the nonlinear term $f_\phi^n := (\Phi_M^n)^2 + \Phi_M^n \phi^n + (\phi^n)^2 - 1$. Thanks to the solution estimates in Lemma 2.2 and (4.4), one applies the discrete embedding inequality (2.1) to find that

$$\begin{aligned} \|f_\phi^n\|_{l^3} &\leq \|\Phi_M^n\|_{l^6}^2 + \|\Phi_M^n\|_{l^6} \|\phi^n\|_{l^6} + \|\phi^n\|_{l^6}^2 + |\Omega_h|^{1/3} \\ &\leq c_\Omega^2 (c_1^2 + c_1 c_2 + c_2^2) + |\Omega_h|^{1/3} = c_3. \end{aligned} \quad (4.11)$$

Multiplying both sides of equation (4.10) by the DOC kernels $\theta_{k-n}^{(k)}$, and summing up n from $n = 2$ to k , we apply the equality (1.10) with $v^j = e^j$ to obtain

$$\nabla_\tau e^k = -\theta_{k-2}^{(k)} b_1^{(2)} \nabla_\tau e^1 + \kappa \sum_{j=2}^k \theta_{k-j}^{(k)} \Delta_h (-\epsilon^2 \Delta_h e^j + f_\phi^j e^j) + \Upsilon_P^k + \Xi_\Phi^k \quad (4.12)$$

for $2 \leq k \leq N$, where Ξ_Φ^k and Υ_P^k are defined by (4.1) and (4.8), respectively. Making the inner product of (4.12) with $2e^k$, and summing k from 2 to n , we obtain

$$\|e^n\|^2 \leq \|e^1\|^2 - 2 \sum_{k=2}^n \theta_{k-2}^{(k)} b_1^{(2)} \|e^k\| \|\nabla_\tau e^1\| + J^n + 2 \sum_{k=2}^n \langle \Upsilon_P^k + \Xi_\Phi^k, e^k \rangle \quad (4.13)$$

for $2 \leq n \leq N$, where J^n is defined by

$$J^n := 2\kappa \sum_{k,j}^{n,k} \theta_{k-j}^{(k)} \langle -\epsilon^2 \Delta_h e^j + f_\phi^j e^j, \Delta_h e^k \rangle. \quad (4.14)$$

Taking $u^j := f_\phi^j$ (with the upper bound $c_u := c_3$), $w^j := e^j$ and $\varepsilon = \epsilon^2$ in Lemma 3.9, one applies the solution bound (4.11) to obtain

$$2\kappa \sum_{k,j}^{n,k} \theta_{k-j}^{(k)} \langle f_\phi^j e^j, \Delta_h e^k \rangle \leq 2\kappa \epsilon^2 \sum_{k,j}^{n,k} \theta_{k-j}^{(k)} \langle \Delta_h e^j, \Delta_h e^k \rangle + \frac{2\kappa c_z^4 c_3^4 m_2^3 m_3^2}{m_1^5 \epsilon^6} \sum_{k=2}^n \tau_k \|e^k\|^2.$$

Then the term J^n in (4.14) can be bounded by

$$J^n \leq \frac{c_\epsilon}{2} \sum_{k=2}^n \tau_k \|e^k\|^2.$$

Therefore, it follows from (4.13) that

$$\|e^n\|^2 \leq \|e^1\|^2 - 2 \sum_{k=2}^n \theta_{k-2}^{(k)} b_1^{(2)} \|e^k\| \|\nabla_\tau e^1\| + \frac{c_\epsilon}{2} \sum_{k=2}^n \tau_k \|e^k\|^2 + 2 \sum_{k=2}^n \|e^k\| \|\Upsilon_P^k + \Xi_\Phi^k\|$$

for $2 \leq n \leq N$. Choosing some integer n_0 ($1 \leq n_0 \leq n$) such that $\|e^{n_0}\| = \max_{1 \leq k \leq n} \|e^k\|$. Taking $n := n_0$ in the above inequality, one can obtain

$$\|e^{n_0}\| \leq \|e^1\| - 2 \|\partial_\tau e^1\| \sum_{k=2}^{n_0} \theta_{k-2}^{(k)} b_1^{(2)} \tau_1 + \frac{c_\epsilon}{2} \sum_{k=2}^{n_0} \tau_k \|e^k\| + 2 \sum_{k=2}^{n_0} \|\Upsilon_P^k + \Xi_\Phi^k\|.$$

By using Lemma 3.1(II), one has

$$-\theta_{k-2}^{(k)} b_1^{(2)} \tau_1 = \tau_1 \prod_{i=2}^k \frac{r_i^2}{1+2r_i} = \tau_k \prod_{i=2}^k \frac{r_i}{1+2r_i} \leq \frac{\tau_k}{2^{k-1}} \quad \text{for } 2 \leq k \leq N,$$

such that

$$-\sum_{k=2}^n \theta_{k-2}^{(k)} b_1^{(2)} \tau_1 \leq \tau \sum_{k=2}^n \frac{1}{2^{k-1}} \leq \tau \quad \text{for } 2 \leq n \leq N.$$

Thus one gets

$$\|e^n\| \leq \|e^{n_0}\| \leq \|e^1\| + 2\tau \|\partial_\tau e^1\| + \frac{c_\epsilon}{2} \sum_{k=2}^n \tau_k \|e^k\| + 2 \sum_{k=2}^n \|\Upsilon_P^k + \Xi_\Phi^k\|.$$

Under the maximum step constraint $\tau \leq 1/c_\epsilon$, we have

$$\|e^n\| \leq 2\|e^1\| + 4\tau \|\partial_\tau e^1\| + c_\epsilon \sum_{k=2}^{n-1} \tau_k \|e^k\| + 4 \sum_{k=2}^n \|\Upsilon_P^k + \Xi_\Phi^k\|.$$

The discrete Grönwall inequality [22, Lemma 3.1] yields the following estimate

$$\|e^n\| \leq 2 \exp(c_\epsilon t_{n-1}) \left(\|e^1\| + 2\tau \|\partial_\tau e^1\| + 2 \sum_{k=2}^n \|\Upsilon_P^k\| + 2 \sum_{k=2}^n \|\Xi_\Phi^k\| \right) \quad \text{for } 2 \leq n \leq N.$$

Furthermore, Lemma 4.1 together with $\|\partial_t^3 \Phi\| = \|I_M \partial_t^3 \Phi\|_{L^2} \leq C_\phi \|\partial_t^3 \Phi\|_{L^2}$, due to Lemma 4.2, gives the bound of the global temporal error term $\sum_{k=2}^n \|\Xi_\Phi^k\|$. Therefore by applying the error estimate (4.8) and the triangle inequality (4.5), we complete the proof. \square

5 Numerical experiments

We run the variable-steps BDF2 scheme (1.7) for the CH equation (1.2). The TR-BDF2 method is always employed to obtain the first-level solution. A simple fixed-point iteration with the termination error 10^{-12} is employed to solve the nonlinear algebra equations at each time level.

5.1 Robustness tests on random time meshes

Example 1. To facilitate the robustness test of the variable-steps BDF2 method (1.7), we consider an exact solution $\Phi(\mathbf{x}, t) = \cos(t) \sin(x) \sin(y)$ with the model parameters $\kappa = 1$ and $\epsilon^2 = 0.5$ by adding a corresponding exterior force on the right hand side of the CH model (1.2).

In the following examinations, the computational domain $(0, 2\pi)^2$ is discretized by using 128^2 spatial meshes. Then the problem is solved until time $T = 1$ on random time meshes. To be more precise, we take the time step sizes $\tau_k := T\sigma_k/S$ for $1 \leq k \leq N$, where $\sigma_k \in (0, 1)$ is the uniformly distributed random number and $S = \sum_{k=1}^N \sigma_k$. Since the spectral accuracy in space is standard, we only test the time accuracy with the numerical error $e(N) := \max_{1 \leq n \leq N} \|\Phi(t_n) - \phi^n\|$ in each run. The numerical order of convergence is estimated by

$$\text{Order} := \frac{\log(e(N)/e(2N))}{\log(\tau(N)/\tau(2N))},$$

Table 1: Accuracy of BDF2 method (1.7) on random time mesh.

N	τ	$e(N)$	Order	$\max r_k$	N_1
40	3.96e-02	1.82e-04	1.69	17.27	3
80	2.44e-02	4.60e-05	2.84	46.22	5
160	1.29e-02	1.16e-05	2.16	167.41	16
320	6.28e-03	2.90e-06	1.93	264.04	29
640	3.05e-03	7.27e-07	1.92	1584.01	62

where $\tau(N)$ denotes the maximum time-step size for total N subintervals.

The numerical results obtained using a set of random meshes are tabulated in Table 1. In addition to the discrete L^2 numerical error between the exact solution and the numerical solution, the maximum time-step size τ , the maximum step ratio $\max r_k$ and the number (denote by N_1) of time levels with the step ratios $r_k \geq 4.864$ are also recorded, respectively.

As observed, the variable-steps BDF2 method (1.7) still achieves the second-order accuracy on arbitrary nonuniform meshes even though some step ratios larger than the update zero-stability limit $r_* \approx 4.864$, see Remark 2. The numerical results indicate that the BDF2 method is much more robust with respect to the step-size variations than previous theoretical predictions. Also, the improved condition $0 < r_k < 4.864$ is still a sufficient condition for second-order convergence. In the following experiments, we always set $r_{\text{user}} = 4$, which is large enough for practical adaptive time-stepping simulations.

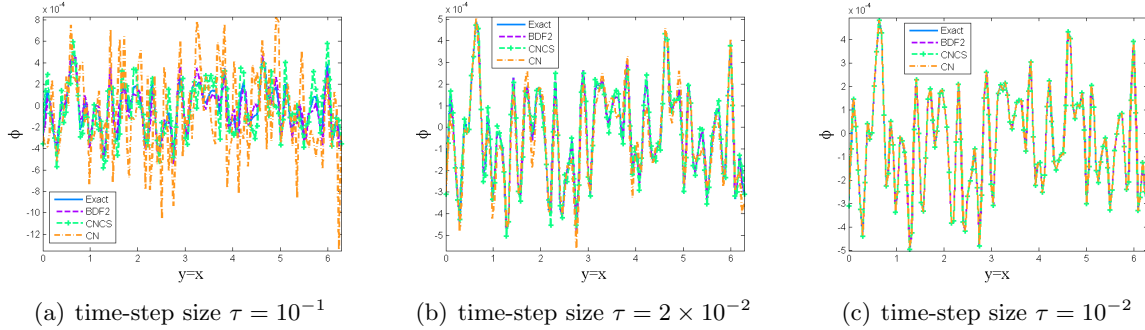


Figure 1: Solution curves by BDF2, CN and CNCS methods at $T = 0.1$.

Example 2. We next simulate the coarsening dynamics of the CH equation (1.2). Precisely, the initial condition is taken as $\Phi_0(\mathbf{x}) = \text{rand}(\mathbf{x})$, where $\text{rand}(\mathbf{x})$ generates random numbers between -0.001 to 0.001 uniformly. Here, the mobility coefficient $\kappa = 0.01$ and the interfacial thickness $\epsilon = 0.05$ are taken in the following numerical simulations. Always, the spatial domain $(0, 2\pi)^2$ is discretized by using 128^2 spatial meshes.

5.2 Numerical comparisons

To further benchmark the BDF2 scheme with the random initial data generated in Example 2, we run several numerical tests to explore the numerical behaviors near the initial time. We also

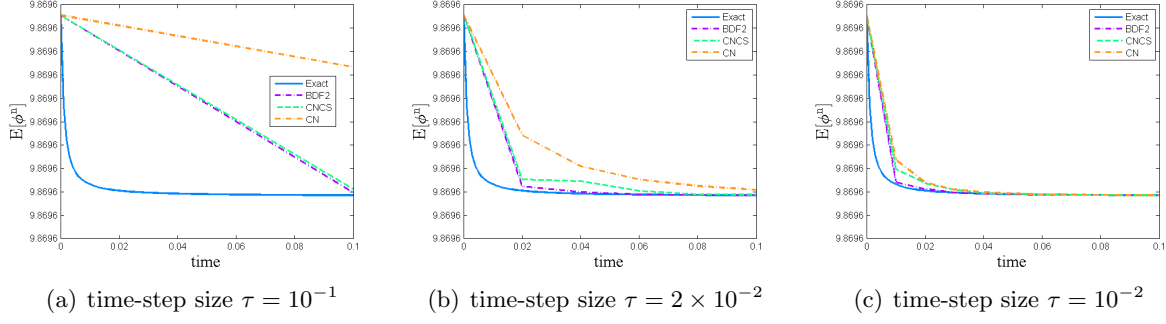


Figure 2: Original energy curves by BDF2, CN and CNCS methods until $T = 0.1$.

implement the unconditionally energy stable Crank-Nicolson (denoted by CN) method [30],

$$\partial_\tau \phi^n = \kappa \Delta_h \mu^{n-\frac{1}{2}} \quad \text{with} \quad \mu^{n-\frac{1}{2}} = \frac{1}{2} [(\phi^n)^2 + (\phi^{n-1})^2] \phi^{n-\frac{1}{2}} - \phi^{n-\frac{1}{2}} - \varepsilon^2 \Delta_h \phi^{n-\frac{1}{2}},$$

and the second-order Crank-Nicolson convex-splitting (denoted by CNCS) method [9],

$$\partial_\tau \phi^n = \kappa \Delta_h \hat{\mu}^{n-\frac{1}{2}} \quad \text{with} \quad \hat{\mu}^{n-\frac{1}{2}} = \frac{1}{2} [(\phi^n)^2 + (\phi^{n-1})^2] \phi^{n-\frac{1}{2}} - \check{\phi}^{n-\frac{1}{2}} - \varepsilon^2 \Delta_h \hat{\phi}^{n-\frac{1}{2}},$$

where $\phi^{n-\frac{1}{2}} := (\phi^n + \phi^{n-1})/2$, $\hat{\phi}^{n-\frac{1}{2}} := (3\phi^n + \phi^{n-2})/4$ and $\check{\phi}^{n-\frac{1}{2}} = (3\phi^{n-1} - \phi^{n-2})/2$. Since the CNCS method requires two initialization steps, a first-order convex-splitting scheme [8] is used here to obtain the first-level solution.

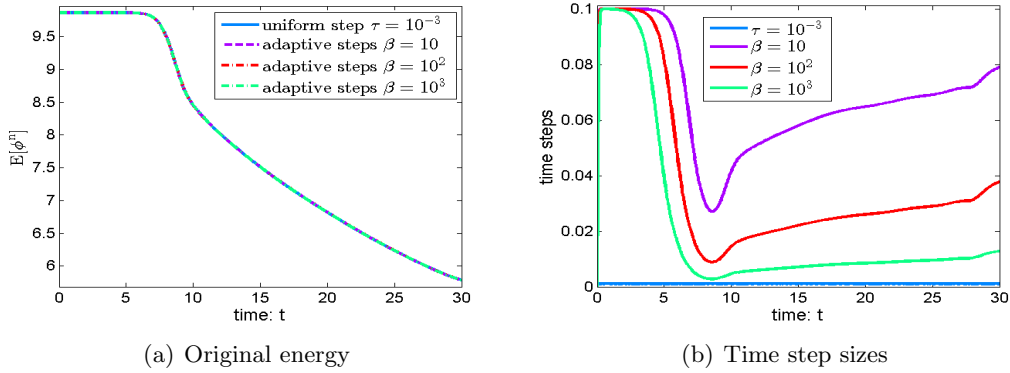


Figure 3: Energy curves and adaptive time-step sizes for different parameters β .

The random initial data initiates a fast coarsening dynamics at the beginning time. We use a random initial profile to test the effectiveness of various numerical methods with different time step sizes. The numerical solution curves are summarized in Figure 1, where the reference solution is obtained by using the BDF2 method with a uniform time-step size $\tau = 10^{-3}$. We observe that solutions of CN and CNCS methods tend to generate non-physical oscillations when some large time steps are used. In contrast, the BDF2 solution is more robust and accurate than the CN and CNCS schemes with the same time step size. It seems that the BDF2 method is more suitable than Crank-Nicolson type schemes when large time-step sizes are adopted.

Table 2: CPU time (in seconds) and total time steps comparisons.

Strategies	$\tau = 10^{-3}$	$\beta = 10$	$\beta = 10^2$	$\beta = 10^3$
CPU time	337.736	13.870	26.568	62.797
Time levels	30000	493	1190	3554

5.3 Simulation of coarsening dynamics

In this subsection, we simulate the coarsening dynamics by using the variable-steps BDF2 method (1.7) with the random initial condition. In what follows, to capture the multiple time scales accurately and to improve the computational efficiency for long-time simulations, the time steps are selected by using the following adaptive time-stepping strategy [16],

$$\tau_{ada} = \max \left\{ \tau_{\min}, \frac{\tau_{\max}}{\sqrt{1 + \beta \|\partial_\tau \phi^n\|^2}} \right\} \quad \text{so that} \quad \tau_{n+1} = \min \{ \tau_{ada}, r_{\text{user}} \tau_n \}, \quad (5.1)$$

where $\|\partial_\tau \phi^n\|$ denotes the change rate between two consecutive time step numerical solutions, $\beta > 0$ is a user chosen parameter, τ_{\max} and τ_{\min} are the predetermined maximum and minimum time steps, respectively.

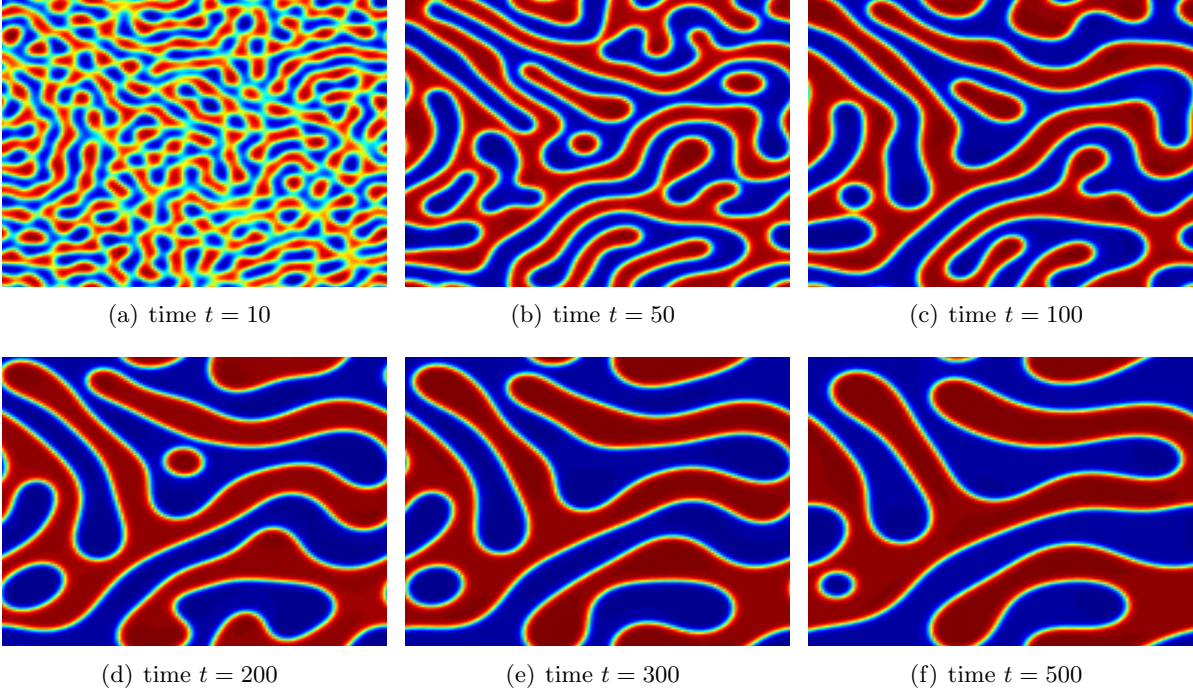


Figure 4: The profile of numerical solution ϕ at different time for the CH model.

We take $\tau_{\min} = 10^{-4}$ and $\tau_{\max} = 10^{-1}$ in the adaptive time-stepping algorithm (5.1), and run the BDF2 method (1.7) until time $T = 30$. The reference solution is obtained by applying a small

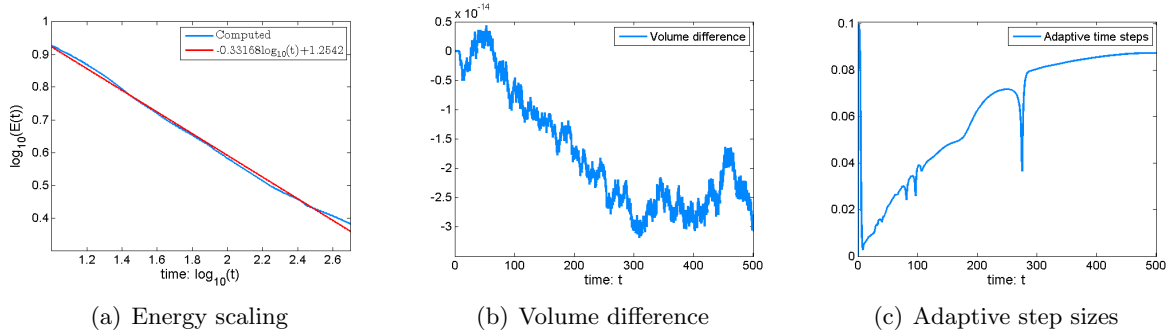


Figure 5: Numerical results show original energy, volume and adaptive time steps of the CH equation during the coarsening dynamics.

time step $\tau = 10^{-3}$. As seen in Figure 3, we use three different user parameters $\beta = 10, 10^2$ and 10^3 to compute the discrete original energy and the corresponding adaptive time-steps. One can observe that the discrete energy curves using the adaptive stepping algorithm are comparable to the reference one. On the other hand, the adjustments of time-steps are closely relied on the user parameter β . As expected, a large β leads to small time-step sizes, and a small β generates large step sizes. The CPU time (in seconds) and the adaptive time levels recorded in Table 2 show the effectiveness and efficiency of the adaptive time-stepping algorithm, which makes the long-time dynamics simulations practical.

We next perform the coarsening dynamic simulations by using the above adaptive time-stepping strategy with the setting $\beta = 10^3$ until time $T = 500$. The evolution of microstructure for the CH model due to the phase separation at different time are summarized in Figure 4. As seen, the microstructure is relatively fine and consists of many precipitations at early time. The coarsening, dissolution, merging processes are also observed. The time evolutions of original energy, volume and the adaptive step sizes are summarized in Figure 5. The subplot (a) of Figure 5 demonstrates a very good agreement with the expected scaling law, i.e., the energy decrease as $O(t^{-\frac{1}{3}})$.

References

- [1] R. ALEXANDER, *Diagonally implicit Runge-Kutta methods for stiff ODEs*, SIAM J. Numer. Anal., 14(6) (1977), pp. 1006–1021.
- [2] J. BECKER, *A second order backward difference method with variable steps for a parabolic problem*, BIT, 38(4) (1998), pp. 644–662.
- [3] A. BERTOZZI, S. ESEDOGLU, AND A. GILLETTE, *Inpainting of binary images using the Cahn-Hilliard equation*, IEEE Trans. Image Process., 16 (2007), pp. 285–291.
- [4] J. CAHN AND J. HILLIARD, *Free energy of a nonuniform system I. interfacial free energy*, J. Chem. Phys., 28 (1958), pp. 258–267.
- [5] K. CHENG, W. FENG, C. WANG, AND S. WISE, *An energy stable fourth order finite difference scheme for the Cahn-Hilliard equation*, J. Comput. Appl. Math., 362 (2019), pp. 574–595.

- [6] K. CHENG, C. WANG, AND S. WISE, *An energy stable BDF2 Fourier pseudo-spectral numerical scheme for the square phase field crystal equation*, Comm. Comput. Phys., 26 (2019), pp. 1335–1364.
- [7] W. CHEN, C. WANG AND X. WANG, *A linear iteration algorithm for a second-order energy stable scheme for a thin film model without slope selection*, J Sci. Comput., 59 (2014), pp. 574–601.
- [8] W. CHEN, X. WANG, Y. YAN AND Z. ZHANG, *A second order BDF numerical scheme with variable steps for the Cahn–Hilliard equation*, SIAM J. Numer. Anal., 57 (1) (2019), pp. 495–525.
- [9] K. CHENG, C. WANG, S. WISE, AND X. YUE, *A second-order, weakly energy-stable pseudo-spectral scheme for the Cahn–Hilliard equation and its solution by the homogeneous linear iteration method*, J. Sci. Comput., 69 (2016), pp. 1083–1114.
- [10] V. Cristini, X. Li, J. Lowengrub, and S. Wise. Nonlinear simulations of solid tumor growth using a mixture model: invasion and branching. *J. Math. Biol.*, 58 (2009), pp. 723–763.
- [11] E. EMMRICH, *Stability and error of the variable two-step BDF for semilinear parabolic problems*, J. Appl. Math. & Computing, 19 (2005), pp. 33–55.
- [12] R.D. GRIGORIEFF, *Stability of multistep-methods on variable grids*, Numer. Math., 42 (1983), pp. 359–377.
- [13] H. GOMEZ AND T. HUGHES, *Provably unconditionally stable, second-order time-accurate, mixed variational methods for phase-field models*, J. Comput. Phys., 230 (2011), pp. 5310–5327.
- [14] E. HAIRER, S.P. NØRSETT AND G. WANNER, *Solving Ordinary Differential Equations I: Nonstiff Problems*, Volume 8 of Springer Series in Computational Mathematics, Second Edition, Springer-Verlag, 1992.
- [15] M.E. HOSEA AND L.F. SHAMPINE, *Analysis and implementation of TR-BDF2*, Appl. Numer. Math., 20 (1996), pp. 21–37.
- [16] J. HUANG, C. YANG, AND Y. WEI, *Parallel energy-stable solver for a coupled Allen–Cahn and Cahn–Hilliard system*, SIAM J. Sci. Comput., 42(5) (2020), pp. C294–C312.
- [17] M.-N. LE ROUX, *Variable step size multistep methods for parabolic problems*, SIAM J. Numer. Anal., 19 (4) (1982), pp. 725–741.
- [18] H.-L. LIAO, B. JI AND L. ZHANG, *An adaptive BDF2 implicit time-stepping method for the phase field crystal model*, IMA J. Numer. Anal., 2020, doi:10.1093/imanum/draa075.
- [19] H.-L. LIAO, X. SONG, T. TANG AND T. ZHOU, *Analysis of the second order BDF scheme with variable steps for the molecular beam epitaxial model without slope selection*, Sci. China Math., 2020, doi:10.1007/s11425-020-1817-4.
- [20] H.-L. LIAO, T. TANG AND T. ZHOU, *On energy stable, maximum-principle preserving, second order BDF scheme with variable steps for the Allen–Cahn equation*, SIAM J. Numer. Anal., 58(4) (2020), pp. 2294–2314.

- [21] H.-L. LIAO, T. TANG AND T. ZHOU, *Positive definiteness of real quadratic forms resulting from variable-step approximations of convolution operators*, arXiv:2011.13383v1, 2020, submitted.
- [22] H.-L. LIAO AND Z. ZHANG, *Analysis of adaptive BDF2 scheme for diffusion equations*, Math. Comp., 2020, DOI: 10.1090/mcom/3585.
- [23] H. NISHIKAWA, *On large start-up error of BDF2*, J. Comput. Phys., 392 (2019), pp. 456–461.
- [24] Z. QIAO, Z. ZHANG AND T. TANG, *An adaptive time-stepping strategy for the molecular beam epitaxy models*, SIAM J. Sci. Comput., 33 (2011), pp. 1395–1414.
- [25] J. SHEN, C. WANG, X. WANG AND S.M. WISE, *Second-order convex splitting schemes for gradient flows with Ehrlich–Schwoebel type energy: application to thin film epitaxy*, SIAM J. Numer. Anal., 50(1) (2012), pp. 105–125.
- [26] J. SHEN, T. TANG, AND L. WANG, *Spectral methods: Algorithms, analysis and applications*, Springer-Verlag, Berlin Heidelberg, 2011.
- [27] G. TUMOLO AND L. BONAVENTURA, *A semi-implicit, semi- Lagrangian, DG framework for adaptive numerical weather prediction*, Quarterly Journal of the Royal Meteorological Society, DOI: 10.1002/qj.2544, 2015.
- [28] W. WANG, Y. CHEN AND H. FANG *On the variable two-step IMEX BDF method for parabolic integro-differential equations with nonsmooth initial data arising in finance*, SIAM J. Numer. Anal., 57(3) (2019), pp. 1289–1317.
- [29] J. XU, Y.K. LI, S.N. WU AND A. BOUSEQUET, *On the stability and accuracy of partially and fully implicit schemes for phase field modeling*, Comput. Methods Appl. Mech. Engrg., 345 (2019), pp. 826–853.
- [30] Z. ZHANG AND Z. QIAO, *An adaptive time-stepping strategy for the Cahn-Hilliard equation*, Comm. Comput. Phys., 11(4) (2012), pp. 1261–1278.